Geophysical and Astrophysical Fluid Dynamics, 2013
Vol. 107, No. 5, 564–586, http://dx.doi.org/10.1080/03091929.2012.751381

Flow of grounded abyssal ocean currents along zonally-varying topography on a rotating sphere

GORDON E. SWATERS†‡*

†Department of Mathematical and Statistical Sciences, Applied Mathematics Institute, University of Alberta, Edmonton, AB, Canada, T6G 2G1
‡Institute for Geophysical Research, University of Alberta, Edmonton, AB, Canada, T6G 2G1

(*Received 2 May 2012; revised 8 October 2012; in final form 8 October 2012; first published online 22 February 2013*)

A steady nonlinear planetary–geostrophic model in spherical coordinates is presented describing the hemispheric-scale meridional flow of grounded abyssal currents on a zonally-sloping bottom. The model, which corresponds mathematically to a quasi-linear hyperbolic partial differential equation, can be solved explicitly for a cross-slope isopycnal field that is grounded (i.e. intersects the bottom on the up slope and down slope sides). As a consequence of the conservation of potential vorticity, the abyssal currents possess decreasing thickness in the equatorward direction while maintaining constant meridional volume transport. There is a small westward zonal transport in the interior of these currents that results in westward intensification as they flow toward the equator. Conditions for the possible formation of a shock to develop on the up slope flank of the current are derived.

Keywords: Grounded abyssal ocean currents; Deep western boundary currents; Planetary–geostrophic balance; Sverdrup vorticity balance; Topographically-steered flow; Spherical geometry

1. Introduction

In a source region of deep water formation, the Sverdrup vorticity balance predicts the equatorward flow of abyssal currents (Stommel and Arons 1960). Away from the source region, however, the Sverdrup vorticity balance cannot infer the flow direction of abyssal currents. Many abyssal currents are characterized by the isopycnal field being grounded against sloping topography (e.g. the deep western boundary undercurrent (DWBC) in the North Atlantic, Richardson 1977). As shown by Nof (1983), a fully grounded abyssal water mass lying over sloping topography on an *f*-plane flows, in the fully nonlinear but reduced-gravity dynamical limit, nondispersively and steadily in the along slope direction, irrespective of the specific height or vorticity field within the abyssal water mass.

*Email: gswaters@ualberta.ca

These two results provide a dynamical scenario for the initiation and maintenance of source-driven grounded abyssal flow over, at least, the mesoscale. That is, in high-latitude regions where deep water is produced (often over sloping topography), the Sverdrup vorticity balance initiates equatorward flow. Once produced, this water mass can become grounded and geostrophically adjusted, maintaining a ''Nof balance'' that permits the possibility of sustained meridional, quasi-steady and coherent abyssal flow away from the source region.

However, the spatial extent of these abyssal currents is well known to be, at least, hemispheric in scale. This raises the question about the role of planetary sphericity in determining the large-scale kinematic structure of these flows. The principal purpose of this paper is to describe some results from a simple, but nevertheless illuminating, reduced-gravity shallow-water model for the meridional, or equatorward, steady flow of grounded abyssal currents on a longitudinally-sloping bottom on a rotating sphere. We note that some preliminary results for a related baroclinic model on a β-plane have been described by Swaters (2006a).

It is important to point out that while we are focused here on one particular aspect of the dynamics of grounded abyssal currents, there are many other processes that are important such as diabatic effects (e.g. Swaters and Flierl 1991), baroclinicity (e.g. Poulin and Swaters 1999), instability (e.g. Swaters 1991, Reszka *et al*. 2002), topographic separation and mixing (e.g. Swaters 1998, 2006a,b). In addition, the model we examine here cannot describe the cross-equatorial flow of grounded abyssal currents where the assumptions of a geostrophically balanced flow must break down (see, e.g. Edwards and Pedlosky 1998a,b, Nof and Borisov 1998, Choboter and Swaters 2003, 2004), or the super-inertial instability associated with frictional super-critical abyssal overflows (e.g. Swaters 2009).

The plan of this paper is as follows. In section 2 the model is derived as an asymptotic reduction of the reduced-gravity shallow water equations in spherical coordinates with variable topography and interpreted as a particular limit of the relevant potential vorticity equation. The model's connection to previously derived nonlinear planetary-wave equations is given.

Section 3 details the general properties of the nonlinear steady-state solutions to the model, which corresponds to a quasi-linear hyperbolic equation with the independent variables given by the latitude and the longitude. The general solution is obtained by the method of characteristics, where it is assumed that the abyssal layer height as a function of longitude is known along a line of constant latitude. It is shown that the characteristics correspond to the streamlines in the flow. It is shown that the position of the groundings (should they occur) do not vary with latitude once set by the boundary condition on the abyssal layer height. It is shown that the net meridional volume transport across the current width is independent of latitude. Conditions for the possible formation of a shock in the solution are derived. In particular, it is shown that if the meridional velocity associated with the boundary condition on the abyssal layer height is everywhere equatorward (for a geometrical configuration corresponding to the flow of abyssal currents along the western edge of an ocean basin, e.g. the western north Atlantic), then no shock will form.

In section 4 an example solution is described in which the abyssal layer height is parabolic in shape and possesses two groundings, one located on the up slope flank and one located on the down slope flank of the current. In this case, the characteristics, i.e. the streamlines can be explicitly determined, is possible to give detailed descriptions of

the along and cross-slope flow pathlines, the abyssal layer height as a function of longitude and latitude, the Eulerian velocity field within the abyssal, the meridional and zonal volume fluxes as well as the meridional and zonal volume transports, respectively. The paper is summarized in section 5.

2. Model derivation

The reduced-gravity shallow-water equations for a stably-stratified abyssal water mass overlying variable bottom topography on a rotating sphere can be written in the form (see, e.g. Vallis 2006)

$$u_t + \frac{uu_\lambda}{R\cos\theta} + \frac{vu_\theta}{R} - \frac{uv\tan\theta}{R} - 2\Omega v\sin\theta = -\frac{g'}{R\cos\theta}(h+h_B)_\lambda, \tag{1a}$$

$$v_t + \frac{uv_\lambda}{R\cos\theta} + \frac{vv_\theta}{R} - \frac{v^2\tan\theta}{R} + 2\Omega u\sin\theta = -\frac{g'}{R}h_\theta, \tag{1b}$$

$$h_t + \frac{1}{R\cos\theta}\left[(hu)_\lambda + (hv\cos\theta)_\theta\right] = 0, \tag{1c}$$

(see figure 1 for the model geometry) where u and v are the zonal (positive eastward) and meridional (positive northward) velocities, respectively, λ is the longitude (positive eastward) and θ is the latitude (positive northward), t is time, Ω is the angular frequency associated with Earth's rotation (2π rads day^{-1}), R is the radius of Earth (about 6300 km), $h(\lambda,\theta,t)$ is the thickness of the abyssal layer, $h_B(\lambda)$ is the longitudinally-varying height of the bottom topography above a constant reference depth and $g' = g(\rho_2-\rho_1)/\rho_2 > 0$ is the (stably-stratified) reduced gravity where ρ_1 and ρ_2 are the densities of the (infinitely deep and motionless) overlying fluid and dynamically active abyssal layer, respectively, and g is the gravitational acceleration (9.81 m s^{-2}). Typical oceanographic values for the reduced gravity are in the range $10^{-4}-10^{-2}$ m s^{-2}.

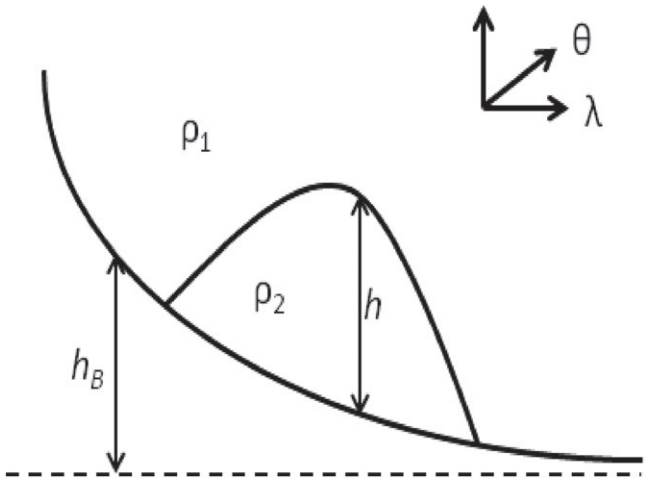

Figure 1. Geometry of the model used in this paper.

The *dynamic* pressure (i.e. the total pressure minus the hydrostatic pressure) in the abyssal layer is given by

$$p = g'\rho_1(h + h_B).$$

The development of the theory presented here for bottom height profiles that vary only longitudinally is done to extract the maximum information possible from an analytically tractable problem. Clearly, in the ''real ocean'' bottom the topography varies longitudinally and meridionally. The effect of these more complex orographies needs further study.

Further analysis is facilitated by introducing the scalings,

$$\lambda = (L/R)\widetilde{\lambda}, \quad t = (R/V)\widetilde{t}, \quad u = (LV/R)\widetilde{u}, \quad v = V\widetilde{v} \tag{2a–d}$$

$$(h, h_B) = \left(2\Omega VL/g'\right)\left(\widetilde{h}, \widetilde{h}_B\right), \quad p = 2\Omega VL\rho_1\,\widetilde{p}, \tag{2e,f}$$

into (1a–c), where the length scale L is a measure of the zonal width of the current, yielding (after dropping the tildes)

$$\varepsilon\delta^2\left(u_t + \frac{uu_\lambda}{\cos\theta} + vu_\theta - uv\tan\theta\right) - v\sin\theta = -\frac{1}{\cos\theta}(h + h_B)_\lambda, \tag{3a}$$

$$\varepsilon\left(v_t + \frac{uv_\lambda}{\cos\theta} + vv_\theta - v^2\tan\theta\right) + u\sin\theta = -h_\theta, \tag{3b}$$

$$h_t + \frac{1}{\cos\theta}\left[(hu)_\lambda + (hv\cos\theta)_\theta\right] = 0, \tag{3c}$$

where ε and δ are, respectively, the Rossby number and aspect ratio given by

$$\varepsilon = \frac{V}{2\Omega L} \quad \text{and} \quad \delta = \frac{L}{R},$$

and where the dynamic pressure is given by

$$p = h + h_B.$$

Assuming typical scales (e.g. Swaters 2006a,b, 2009) of

$$V \simeq 1 \times 10^{-2}\,\text{m/s}, \quad L \simeq 10^5\,\text{m} \quad \text{and} \quad g' \simeq 1 \times 10^{-3}\,\text{m/s}^2,$$

suggests that

$$\varepsilon \simeq 6.9 \times 10^{-4} \quad \text{and} \quad \delta \simeq 1.6 \times 10^{-2},$$

with the additional time, zonal velocity and abyssal height scalings given by, respectively,

$$\frac{R}{V} \simeq 20\ \text{years}, \quad \frac{LV}{R} \simeq 1.6 \times 10^{-4}\ \text{m/s} \quad \text{and} \quad \frac{2\Omega VL}{g'} \simeq 145\,\text{m}.$$

Thus, to leading order in the Rossby number, the model reduces to

$$u = -\frac{1}{\sin\theta}h_\theta, \quad v = \frac{1}{\sin\theta\cos\theta}(h + h_B)_\lambda, \tag{4a,b}$$

$$\sin^2\theta\, h_t + \tan\theta\, h_{B_\lambda} h_\theta - h\, h_\lambda = h_{B_\lambda} h. \tag{4c}$$

Equations (4a–c) correspond to a planetary–geostrophic model in which the velocities are geostrophically determined but for which order-one dynamic variations in the thickness in the abyssal layer are permitted, i.e. the abyssal layer height field can intersect the bottom allowing for groundings (this is similar to the "intermediate" dynamical regime identified by Charney and Flierl (1981)). It is important to point out that the model is singular at the equator ($\theta = 0$), and thus cannot be used to described inter-hemispheric or cross-equatorial flow. The dynamic pressure $p = h + h_B$ forms the geostrophic stream function for the flow as seen in (4a,b).

Equation (4c) is simply the potential vorticity equation for the model. Neglecting terms of $O(\varepsilon)$, the potential vorticity equation associated with (3a–c) is given by

$$\left[\partial_t + (u, v)\cdot\left(\frac{1}{\cos\theta}\partial_\lambda, \partial_\theta\right)\right]\left(\frac{\sin\theta}{h}\right) = 0,$$

and if (4a,b) are substituted in for u and v, respectively, one obtains (4c). Alternatively, equation (4c) may be interpreted as a variant of the so-called *planetary geostrophic wave equation* introduced by Anderson and Killworth (1979), Dewar (1987), Wright and Willmott (1992) and Edwards *et al.* (1998), generalized to spherical geometry with variable bottom topography.

One useful property of the model (4a–c) is that it ensures that the appropriate kinematic condition associated with a grounding is automatically satisfied. That is, one does not need to apply the kinematic boundary condition as an additional auxiliary external constraint since the solution to (4c) necessarily will satisfy it. To see this, suppose that a grounding occurs along the potentially time-dependent curve $\lambda = \widetilde{\lambda}(\theta, t)$, i.e. $h\big(\widetilde{\lambda}, \theta, t\big) = 0$. The appropriate kinematic boundary condition that needs to be satisfied can be written in the form

$$\left[\partial_t + (u, v)\cdot\left(\frac{1}{\cos\theta}\partial_\lambda, \partial_\theta\right)\right]\Big(\widetilde{\lambda}(\theta, t) - \lambda\Big) = 0 \quad \text{evaluated on} \quad \lambda = \widetilde{\lambda}(\theta, t),$$

which reduces to

$$\widetilde{\lambda}_t + \frac{h_\theta}{\sin\theta\cos\theta} + \frac{(h + h_B)_\lambda \widetilde{\lambda}_\theta}{\sin\theta\cos\theta} = 0 \quad \text{evaluated on} \quad \lambda = \widetilde{\lambda}(\theta, t).$$

However, it follows from $h\big(\widetilde{\lambda}, \theta, t\big) = 0$ that

$$h_t + h_\lambda \widetilde{\lambda}_t = 0 \quad \text{evaluated on} \quad \lambda = \widetilde{\lambda}(\theta, t),$$

and

$$h_\theta + h_\lambda \widetilde{\lambda}_\theta = 0 \quad \text{evaluated on} \quad \lambda = \widetilde{\lambda}(\theta, t),$$

which therefore implies that

$$\frac{h_t}{h_\lambda} - \frac{h_\theta}{\sin\theta\cos\theta} + \frac{(h + h_B)_\lambda h_\theta}{\sin\theta\cos\theta\, h_\lambda} = 0 \quad \text{evaluated on} \quad \lambda = \widetilde{\lambda}(\theta, t),$$

which simplifies to

$$h_t + \frac{h_{B\lambda} h_\theta}{\sin\theta\cos\theta} = 0 \quad \text{evaluated on} \quad \lambda = \widetilde{\lambda}(\theta, t),$$

but this is identical to (4c) evaluated on the *grounding* $\lambda = \widetilde{\lambda}(\theta, t)$. Thus, no additional boundary conditions are needed to ensure that the solutions of (4a–c) will satisfy the appropriate kinematic boundary condition on a grounding. This property is very convenient when constructing numerical solutions (Swaters 1998, 2006b).

3. Steady state solution

We describe the equilibrium solution to the model (4a–c) in which $h(\lambda, \theta)$ will be determined by the steady-state quasi-linear hyperbolic equation

$$\tan\theta\, h_\theta - \frac{h}{h_{B_\lambda}}\, h_\lambda = h. \tag{5a}$$

The model (5a) can be solved using the method of characteristics with the boundary condition

$$h(\lambda, \theta_0) = h_0(\lambda), \tag{5b}$$

where θ_0 is a given reference latitude and $h_0(\lambda)$ is a prescribed abyssal height profile that varies only in the longitudinal or zonal direction. It is remarked that the boundary height profile is ''grounded'' if there exists λ_* for which $h_0(\lambda_*) = 0$.

The solution to (5a) subject to (5b) can be written in the form (see the Appendix for details)

$$h(\lambda, \theta) = \frac{\sin\theta}{\sin\theta_0} h_0(\tau), \tag{6a}$$

$$h_B(\tau) + \frac{\sin\theta_0 - \sin\theta}{\sin\theta_0} h_0(\tau) = h_B(\lambda). \tag{6b}$$

Given λ and θ, one solves (6b) for $\tau\,(\lambda, \theta)$ (note that $\tau\,(\lambda, \theta_0) = \lambda$) and then determines $h(\lambda, \theta)$ from (6a). In the case where $h_{B_\lambda} < 0$ (as would be the case along the western boundary of an ocean basin), the solution describes predominately equatorward flow with λ ranging over the set of longitudes for which $h > 0$ (i.e. the *support* of h) and the *maximum* latitudinal extent is $0 < \theta \le \theta_0$ in the northern hemisphere or $\theta_0 \le \theta < 0$ in the southern hemisphere. In the case where $h_{B_\lambda} > 0$ (as would be the case along the eastern boundary of an ocean basin), the solution describes (predominately) poleward flow and the *maximum* latitudinal extent possible is $\pi/2 > \theta \ge \theta_0 > 0$ in the northern hemisphere or $-\pi/2 < \theta \le \theta_0 < 0$ in the southern hemisphere.

It is important to emphasize that we are considering a highly idealized ''process'' model with many simplifying assumptions including meridionally-aligned topography without variations with respect to latitude and a domain without impenetrable barriers stopping or obstacles blocking the flow located at some latitude. Notwithstanding these restrictive idealizations, we suggest that the properties associated with the solution will, nevertheless, be relevant in understanding important aspects of the basin-scale kinematic structure of grounded abyssal flow on a rotating sphere that occurs in the ocean along more-or-less meridionally-aligned continental boundaries.

3.1. *Properties of the solution*

The first thing to note is that the abyssal layer height monotonically decreases in the equatorward direction. In the limit as $\theta \to 0$, it follows from (6a) that $h(\lambda, \theta) \to 0$. This is a straightforward consequence of the fact that the potential vorticity, which for the planetary–geostrophic approximation assumed here is given by $\sin\theta/h$, is a Lagrangian invariant of the motion. Thus, following the geostrophic motion as θ approaches the equator, h must decrease to zero.

The characteristics associated with the quasi-linear model (5a) are the curves in (λ, θ)-space along which τ is constant, as determined by (6b). Along these characteristic curves

$$\left.\frac{\mathrm{d}\theta}{\mathrm{d}\lambda}\right|_{\tau=\text{constant}} = -\frac{h_B'(\lambda)\sin\theta_0}{\cos\theta\, h_0(\tau)}. \tag{7}$$

In order to be specific in our discussion, we describe the physical situation where $h_B'(\lambda) < 0$ with $\theta > 0$ corresponding to predominately equatorward flow in the northern hemisphere along a topographic slope in which the depth of the ocean increases as λ increases, i.e. eastward. This is a model for the equatorward flow of a grounded abyssal water mass along a continental slope on the western side of an ocean basin. In this situation the characteristics are, generally speaking, aligned in the southwest to the northeast direction since

$$\frac{h_B'(\lambda)\sin\theta_0}{\cos\theta\, h_0(\tau)} < 0 \Longrightarrow \left.\frac{\mathrm{d}\theta}{\mathrm{d}\lambda}\right|_{\tau=\text{constant}} > 0.$$

The characteristics overlie, that is, are co-parallel to, the geostrophic streamlines. Equations (6a,b) imply

$$p(\lambda, \theta) \equiv h_B(\lambda) + h(\lambda, \theta) = h_B(\tau) + h_0(\tau). \tag{8}$$

Thus, when τ is constant, i.e. along a characteristic, the geostrophic pressure/stream function is constant and the characteristics coincide with the streamlines. The characteristics, therefore, describe the path lines in the flow and given the orientation of the characteristics associated with (7) when $h_B'(\lambda) < 0$ with $\theta > 0$, the equatorward flow is, generally speaking, moving in the northeast to the southwest direction as it is, nevertheless, topographically-steered equatorward along the sloping bottom.

The corresponding velocity components, determined by (4a,b) are given by, respectively

$$\begin{aligned} u(\lambda, \theta) = -\frac{p_\theta}{\sin\theta} &= -\frac{\left[h_B'(\tau) + h_0'(\tau)\right]\tau_\theta}{\sin\theta} \\ &= -\frac{\cot\theta\, h_0(\tau)\left[h_B'(\tau) + h_0'(\tau)\right]}{\sin\theta_0\, h_B'(\tau) + (\sin\theta_0 - \sin\theta)h_0'(\tau)}, \end{aligned} \tag{9a}$$

$$\begin{aligned} v(\lambda, \theta) = \frac{p_\lambda}{\sin\theta\cos\theta} &= \frac{\left[h_B'(\tau) + h_0'(\tau)\right]\tau_\lambda}{\sin\theta\cos\theta} \\ &= \frac{\sin\theta_0\, h_B'(\lambda)\left[h_B'(\tau) + h_0'(\tau)\right]}{\sin\theta\cos\theta\left[\sin\theta_0\, h_B'(\tau) + (\sin\theta_0 - \sin\theta)h_0'(\tau)\right]}, \end{aligned} \tag{9b}$$

where (6b) and (8) have been used and the "prime" means differentiation with respect to the argument. Observe that as $\theta \to 0$, both u and v become unbounded as a

consequence of the fact that the geostrophic balance (4a,b) breaks down at the equator. The meridional and zonal volume fluxes given by vh and uh, respectively, however remain bounded over the entire domain (including at the equator).

Another general property of the solution is that the position of the groundings in the abyssal height field, that is, the location(s) where $h(\lambda,\theta)=0$, i.e. h intersects the bottom, are invariant with respect to θ once set by their location in the boundary condition (5b). This means that throughout the domain the groundings will simply correspond to the fixed λ-values for which $h_0(\lambda)=0$. To see this suppose that a grounding in the solution occurs along the curve $\lambda=\widetilde{\lambda}(\theta)$ (allowing for a possible θ-dependence). It follows from (6a) that

$$h\big(\widetilde{\lambda}(\theta),\theta\big)=0=\frac{\sin\theta}{\sin\theta_0}h_0\Big(\tau\big(\widetilde{\lambda}(\theta),\theta\big)\Big)\Longrightarrow h_0\Big(\tau\big(\widetilde{\lambda}(\theta),\theta\big)\Big)=0. \tag{10a}$$

But it therefore follows from (6b) that

$$h_B\Big(\tau\big(\widetilde{\lambda}(\theta),\theta\big)\Big)=h_B\big(\widetilde{\lambda}(\theta)\big)\Longrightarrow\tau\big(\widetilde{\lambda},\theta\big)=\widetilde{\lambda}, \tag{10b}$$

since $h_0\big(\tau\big(\widetilde{\lambda},\theta\big)\big)=0$. Thus, along a grounding we necessarily have $\lambda=\widetilde{\lambda}$ and $\tau\big(\widetilde{\lambda},\theta\big)=\widetilde{\lambda}$, where $h_0\big(\widetilde{\lambda}\big)=0$, i.e. the λ-location of a grounding is independent of θ and is set by the boundary data along $\theta=\theta_0$. Since the value of τ is constant along a grounding, the groundings correspond to a characteristic and, therefore, also correspond to a streamline in the flow.

Since the location of the groundings are fixed and do not vary with respect to θ, it necessarily follows that the kinematic condition along the grounding $\lambda=\widetilde{\lambda}$ is simply $u\big(\widetilde{\lambda},\theta\big)=0$. We see that this automatically follows from (9a), as it must, since $h_0\big(\tau\big(\widetilde{\lambda},\theta\big)\big)=h_0\big(\widetilde{\lambda}\big)=0$.

We hasten to add that the above argument is explicitly dependent on the solution being given by (6a,b). Should it be the case that, for example, that a shock develops along a grounding at a specific latitude (see the example in the next section), it is possible that the location of the grounding begins to shift zonally after the shock has formed.

The fact that the location of the groundings does not vary with latitude θ, together with the fact, as previously established, that the streamlines are oriented in the northeast to the southwest direction (when $h_B'(\lambda)<0$ with $\theta>0$) means that the flow exhibits a westward intensification, i.e. as the flow moves equatorward the streamlines shift westward or in the onshore or in the up slope direction. In fact, as shown below, it is possible, depending on the boundary condition along $\theta=\theta_0$ for a "shock" to form in the solution on the up slope or western flank. The formation of such a shock could result in mixing between the abyssal water mass and the overlying water column on the up slope flank of the abyssal current as it propagates equatorward. This would be a decidedly different "instability mechanism" than baroclinic destabilization, which preferentially occurs on the down slope or offshore side of grounded abyssal currents (Swaters 1991, 1998, 2006a,b).

The *net* meridional volume transport is also constant with respect to θ. Suppose that the abyssal current height $h_0(\lambda)$ is only nonzero in the region $\lambda_1<\lambda<\lambda_2$, i.e. $h_0(\lambda)>0$ only for $\lambda\in(\lambda_1,\lambda_2)$ with $h_0(\lambda_{1,2})=0$ (such as shown in figure 1). The net

(nondimensional) *meridional* volume transport as a function of θ, denoted by $T_m(\theta)$, is given by

$$\begin{aligned} T_m(\theta) &\equiv \int_{\lambda_1}^{\lambda_2} h(\lambda,\theta)\, v(\lambda,\theta)\, \cos\theta \,\mathrm{d}\lambda = \int_{\lambda_1}^{\lambda_2} \frac{h\,(\lambda,\theta)\, p_\lambda(\lambda,\theta)}{\sin\theta}\,\mathrm{d}\lambda \\ &= \frac{1}{\sin\theta_0}\int_{\lambda_1}^{\lambda_2} h_0(\tau)[h_0(\tau)+h_B(\tau)]_\tau \tau_\lambda \,\mathrm{d}\lambda \\ &= \frac{1}{\sin\theta_0}\int_{\tau(\lambda_1,\,\theta)}^{\tau(\lambda_2,\,\theta)} h_0(\tau)\big[h_0'(\tau)+h_B'(\tau)\big]\,\mathrm{d}\tau = \frac{1}{\sin\theta_0}\int_{\lambda_1}^{\lambda_2} h_0(\tau)h_B'(\tau)\mathrm{d}\tau, \end{aligned} \tag{11}$$

which is independent of θ, where (6a,b), (8) and (10b) (noting that $\tau(\lambda_{1,2},\theta)=\lambda_{1,2}$) and the fact that $h_0(\lambda_{1,2})=0$ have been used.

Finally, it is remarked that the properties just described implicitly assume, of course, that the solution as written in the form given by (6a,b) is valid. However, since the underlying model (4c) is a quasi-linear hyperbolic equation, it is possible that a shock could develop in the solution for some value of θ and λ in the domain of interest and generically this is to be expected. In this case, the solution (6a,b) does not describe the abyssal layer height equatorward of the latitude at which the shock forms.

3.2. *Possible formation of a shock*

As discussed previously, the westward intensification of the streamlines or characteristics as the flow moves equatorward (when $h_B'(\lambda)<0$) could result in shock formation on the western flank of the propagating abyssal water mass. The formation of a shock in the solution will correspond to the first θ-value (as θ decreases from $\theta_0>0$) where $|h_\lambda|\to\infty$ (assuming flow in the northern hemisphere with $h_B'(\lambda)<0$). From (6a) it follows that

$$h_\lambda(\lambda,\theta) = \frac{\sin\theta}{\sin\theta_0}h_0'(\tau)\,\tau_\lambda = \frac{\sin\theta\, h_0'(\tau)\, h_B'(\lambda)}{\sin\theta_0\, h_B'(\tau)+(\sin\theta_0-\sin\theta)h_0'(\tau)}, \tag{12}$$

where (6b) has been used. Thus, a shock will occur for the first value of $0<\theta\le\theta_0$ (for equatorward flow in the northern hemisphere) for which

$$\sin\theta = \left[\frac{h_0'(\tau)+h_B'(\tau)}{h_0'(\tau)}\right]\sin\theta_0,$$

which we denote by θ_s, and is given by

$$\sin\theta_s = \max_\tau\left[\frac{h_0'(\tau)+h_B'(\tau)}{h_0'(\tau)}\,\middle|\, h_0'(\tau)>0\right]\sin\theta_0, \tag{13}$$

where we assume $h_B'(\tau)<0$. If $h_B'(\tau)<0$, the shock, if it develops, can only occur on the up slope side of the abyssal current height profile where $h_0'(\tau)>0$ so that $\theta_s<\theta_0$. Note that if $h_0'(\tau)$ and $h_B'(\tau)<0$, then necessarily $\big[h_0'(\tau)+h_B'(\tau)\big]/h_0'(\tau)>1$ implying that $\theta_s>\theta_0$, which is not physically relevant.

Should it be the case that

$$\max_{\tau}\left[\frac{h_0'(\tau)+h_B'(\tau)}{h_0'(\tau)}\middle| h_0'(\tau)>0\right]<0,$$

then, formally, $\theta_s<0$ and this is not physically relevant either since the solution is singular at the equator $\theta=0$ and cannot be extended into the southern hemisphere where $\theta<0$ in any event. In this case, then, *no* shock develops in the domain of interest $\theta>0$ (i.e. the northern hemisphere).

We can give a simple physical interpretation for this result. The meridional velocity associated with the abyssal layer height profile along $\theta=\theta_0$ is given by

$$v(\lambda,\theta_0)=\frac{h_B'(\lambda)+h_0'(\lambda)}{\sin\theta_0\cos\theta_0}.$$

Thus,

$$h_B'(\lambda)+h_0'(\lambda)<0\Longleftrightarrow v(\lambda,\theta_0)<0.$$

Consequently, if the meridional flow associated with the abyssal layer height profile along $\theta=\theta_0$ is everywhere equatorward, no shock will form in the solution. We note that this "no shock condition" is similar to the condition, derived by Nof *et al.* (2002), for the stability of an outflow on a continental slope.

Thus, the only physically relevant possibility for a shock to occur is when

$$0<\max_{\tau}\left[\frac{h_0'(\tau)+h_B'(\tau)}{h_0'(\tau)}\middle| h_0'(\tau)>0\right]<1,$$

or, equivalently, if there exists a point where the meridional velocity, associated with the abyssal layer height profile along $\theta=\theta_0$, is poleward then a shock will form. If this condition holds then a shock forms on the up slope or western flank of the equatorward propagating abyssal water mass (in the northern hemisphere) and the potential for mixing by nonbaroclinic instability processes can develop. Conceptually, we can see why a shock will form in this case. In the region of poleward flow, (7) implies that the flow moves (in the northern hemisphere) from the southwest to the northeast. But in the region of equatorward flow, (7) implies that the flow moves (in the northern hemisphere) from the northeast to the southwest. As these flow patterns converge, it is possible that the cross slope gradient $h_\lambda(\lambda,\theta)$ can be become unbounded.

If we denote τ_s as the maximizer, i.e.

$$\max_{\tau}\left[\frac{h_0'(\tau)+h_B'(\tau)}{h_0'(\tau)}\middle| h_0'(\tau)>0\right]\Longrightarrow\tau=\tau_s, \tag{14}$$

then the longitude associated with the point of shock formation, denoted by λ_s, is determined by (6b), i.e.

$$h_B(\lambda_s)=h_B(\tau_s)+\frac{\sin\theta_0-\sin\theta_s}{\sin\theta_0}h_0(\tau_s). \tag{15}$$

Assuming a shock forms at (λ_s,θ_s) where $0<\theta_s<\theta_0$ (in the northern hemisphere), it is possible to formally extend the solution equatorward be "inserting" a discontinuity for $h(\lambda,\theta)$ along the curve, denoted by $\lambda=\Gamma(\theta)$, in the region $0<\theta<\theta_s$ determined by the

Rankine–Hugoniot condition associated with (5a). In conservation balance form, (5a) can be written as

$$h_\theta + \left(-\frac{h^2}{2\tan\theta\, h_{B_\lambda}}\right)_\lambda = \frac{h}{\tan\theta}\left(1 + \frac{h_{B_{\lambda\lambda}} h}{2\left(h_{B_\lambda}\right)^2}\right). \tag{16}$$

Assuming smoothly varying topography, the Rankine–Hugoniot condition associated with (16) therefore implies that $\Gamma(\theta)$ is the solution to the initial-value problem

$$\frac{\mathrm{d}\Gamma}{\mathrm{d}\theta} = -\frac{h^+(\Gamma,\theta) + h^-(\Gamma,\theta)}{2\tan\theta\, h_{B_\lambda}(\Gamma)} \quad \text{subject to} \quad \Gamma(\theta_s) = \lambda_s, \tag{17}$$

where $h^+(\Gamma,\theta)$ and $h^-(\Gamma,\theta)$ are $h(\lambda,\theta)$ (with $\lambda = \Gamma(\theta)$) evaluated to the east and to the west, respectively, of the shock.

Care must be taken in determining the geostrophic velocity (9a,b) in the pre- and post-shock formation regions. In the pre-shock formation region the velocity will be determined by (9a,b). Once a shock forms, however, it will follow that u and v will be determined by (9a,b) away from the shock but will be undefined along $\Gamma(\theta)$. At the point of shock formation $|v| \to \infty$ (and possibly $|u| \to \infty$ depending on whether or not the shock initiation occurs along a grounding). We would argue that this post-shock structure for the velocity field is not physical and additional physics is required (e.g. time dependence, dissipation or mixing) to determine the velocity at and near $\Gamma(\theta)$. In any event, we would assert that realistically, one should expect that $v(\lambda,\theta_0) < 0$ for all λ (in the northern hemisphere with $h_{B_\lambda} < 0$) and so a shock would never occur.

4. Example solution

In order to illustrate the theory, we take

$$h_B(\lambda) = -s(\lambda - 5a/4), \tag{18a}$$

$$h_0(\lambda) = \begin{cases} H\left(1 - \lambda^2/a^2\right) & \text{for } |\lambda| < a, \\ 0 & \text{for } |\lambda| > a, \end{cases} \tag{18b}$$

where $s > 0$, $H > 0$, $a > 0$ and $\theta_0 > 0$ (the longitudinal or zonal shift in (18a) of $-5a/4$ is without loss of generality and is done for graphical convenience only). This configuration will correspond to predominately equatorward flow in the northern hemisphere in which the bottom topography slopes linearly downward in the eastward direction and the boundary abyssal height profile along $\theta = \theta_0$ is parabolic in shape with maximum height H located at $\lambda = 0$ and possesses two groundings; an up slope or western grounding located at $\lambda = -a$ and a down slope or eastern grounding located at $\lambda = a$.

The solution for $h(\lambda,\theta)$ is determined by (6a,b) will therefore be given by

$$h(\lambda,\theta) = \frac{\sin\theta}{\sin\theta_0} \times \begin{cases} H\left(1 - \tau^2/a^2\right) & \text{for } |\tau| < a, \\ 0 & \text{for } |\tau| > a, \end{cases} \tag{19a}$$

with $\tau\,(\lambda,\theta)$ given by

$$\tau(\lambda,\theta)=\begin{cases}\mathcal{D} & \text{for } |\lambda|<a,\\ \lambda & \text{for } |\lambda|>a,\end{cases} \tag{19b}$$

where

$$\mathcal{D}(\lambda,\theta)=\frac{-s+\sqrt{s^2+4H(\sin\theta_0-\sin\theta)[s\lambda+H(\sin\theta_0-\sin\theta)/\sin\theta_0]/(a^2\sin\theta_0)}}{2H(\sin\theta_0-\sin\theta)/(a^2\sin\theta_0)}, \tag{19c}$$

and (19b,c) has been obtained by explicitly solving for τ from (6b). The statement $\tau=\lambda$ for $|\lambda|>a$ in (19b,c) is vacuous since $h_0(\lambda)=0$ for $|\lambda|>a$, i.e. the characteristics carry no information since the solution is identically zero in the region $|\lambda|>a$. It follows from (19b,c) that $\tau\to\lambda$ as $\theta\to\theta_0$ (this is the reason why the plus sign is chosen in the quadratic formula in the solution for τ from (6b)). The solution given by (19–c) will be valid in the region $0<\theta_s<\theta\le\theta_0$.

It follows from (13), (18a,b) that, formally, a shock will form in this solution at latitude $\theta=\theta_s$ given by

$$\sin\theta_s=\left(1+\max_{\tau}\left[\frac{sa^2}{2H\tau}\right|-a\le\tau<0\right]\right)\sin\theta_0, \tag{20}$$

which implies that

$$\tau_s=-a, \tag{21}$$

which in turn implies that

$$\sin\theta_s=\left(1-\frac{sa}{2H}\right)\sin\theta_0. \tag{22}$$

Consequently, if

$$\frac{sa}{2H}\ge 1, \tag{23}$$

no shock will form since if (23) holds it follows, formally, that $\theta_s\le 0$, which is outside the region of applicability of the model. We therefore conclude that increasing the bottom slope or width (i.e. the longitudinal extent) or decreasing the maximum height of the abyssal water mass inhibits shock formation, whereas decreasing the bottom slope or width or increasing the maximum height of the abyssal water mass promotes shock formation.

If the quantities in (23) are replaced with their dimensional or unscaled analogues as defined in (2a–f), but here denoted by an asterisk, then

$$\frac{s^*a^*}{2}\ge H^*, \tag{24}$$

where $a^*\equiv aL\cos\theta_0$ and $H^*\equiv(2\Omega VL/g')\ H$ are in metres and $s^*\equiv 2\Omega V/(g'\cos\theta_0)\ s$ is dimensionless and expressed in units of metres/metres. Typical scales associated with the DWBC in midlatitudes suggest $s^*\sim 5.6\times10^{-3}$ and $a^*\sim 100\,\text{km}$, so that in these circumstances, condition (24) suggests that if $H^*\lesssim 420\,\text{m}$, no shock will form. The value of the bottom slope s^* used above is taken from figure 2(a) in Swaters (2006a), which

was computed by averaging the observed topography in the western North Atlantic from 20° to 60° N.

Alternatively, as suggested by (13), expression (23) can be interpreted as the ratio of the bottom slope (s) to the maximum longitudinal or cross-topographic slope of the boundary height profile in (18b), given by $2H/a$. If the bottom slope exceeds the maximum longitudinal slope in the boundary height profile, then no shock will form. As argued previously, we can give an interpretation of the condition (23) in terms of the along-slope geostrophic velocity along $\theta = \theta_0$. Condition (23) can be written in the form

$$-s + \frac{2H}{a} \leq 0 \Longleftrightarrow \max_{\tau}\left[h_B'(\tau) + h_0'(\tau)\right] \leq 0 \Longleftrightarrow \max_{\lambda} v|_{\theta=\theta_0} \leq 0, \tag{25}$$

where (4b) has been used. Then, from (25), no shock will form in the solution if the velocity is everywhere equatorward along $\theta = \theta_0$. Should the boundary abyssal height profile be such that there existed a poleward velocity somewhere along $\theta = \theta_0$, then a shock will form in the water abyssal mass before it reaches the equator (this qualitative description is also applicable to flow in the southern hemisphere).

In order to visualize the solution we need to pick specific values for θ_0, H, a and s. To begin with, we will choose $\theta_0 = \pi/3$ (i.e. we will "initialize" the solution along 60° N; this choice of latitude is not necessary and is only done for graphical convenience). We assume that $H \simeq 1.38$ (corresponding to a *dimensional* maximum thickness of the abyssal current of about 200 m along $\theta = \theta_0$, $a = 2.0$ (corresponding to an average *dimensional* cross-slope half width of about 170 km for the abyssal current over the interval $0 < \theta < \theta_0$) and $s \simeq 1.92$ (corresponding to a topographic slope of about 5.6×10^{-3} in Cartesian (m/m) units along $\theta = \theta_0$. These values satisfy (23), i.e. $sa/(2H) \simeq 1.4$, i.e. the flow is everywhere equatorward along $\theta = \theta_0$, so that no shock will form in the solution in the region $0 < \theta < \theta_0$.

Figure 2 is a graph of the abyssal layer height $h_0(\lambda)$ and topographic profile $h_B(\lambda)$ as given by (18a,b), respectively, versus λ, along $\theta = \theta_0$. At its maximum, located at $\lambda = 0$, the thickness of the abyssal water layer is, dimensionally, about 200 m. Across the zonal

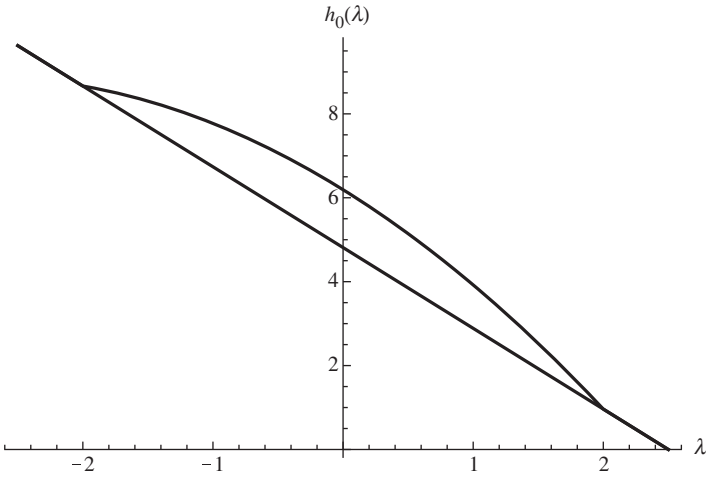

Figure 2. Abyssal height profile $h_0(\lambda)$ along $\theta = \theta_0$.

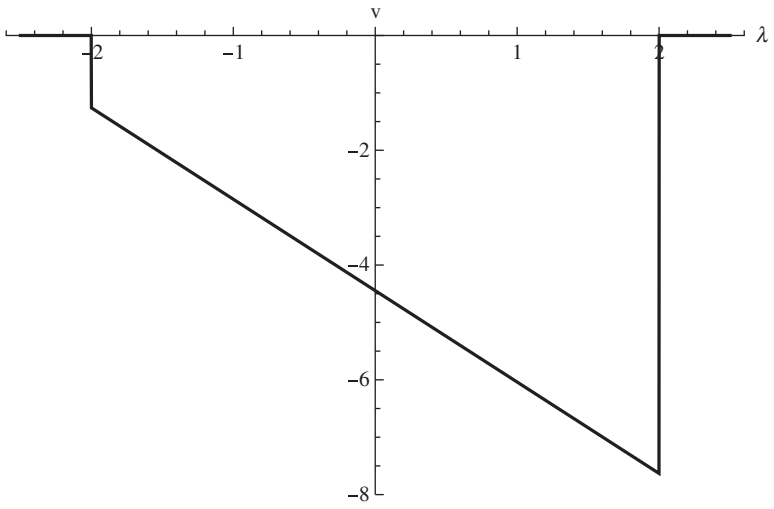

Figure 3. Meridional velocity profile $v(\lambda, \theta)$ along $\theta = \theta_0$.

extent of the abyssal layer water mass, which is about 340 km, the mean depth of the ocean has increased by about 1.9 km due to the linearly varying bottom topography.

Within the abyssal current, the velocity is everywhere equatorward (as it must since (23) is satisfied). This is shown in figure 3, which is a graph of the meridional velocity $v(\lambda, \theta_0)$ versus λ as determined by (9b), i.e.

$$v(\lambda, \theta_0) = \frac{h'_B(\lambda) + h'_0(\lambda)}{\sin\theta_0 \cos\theta_0} = -\frac{s + 2H\lambda/a^2}{\sin\theta_0 \cos\theta_0}, \quad \text{for } |\lambda| < a, \tag{26}$$

and is not defined for $|\lambda| > a$. The meridional velocity linearly decreases as λ increases. It follows from (26) that the maximum meridional velocity occurs for $\lambda = -a$ and if (23) holds (as it does for our choice of parameter values), then the maximum meridional velocity is strictly negative (i.e. equatorward) as shown in figure 3. The maximum current speed occurs on the down slope edge, i.e. $\lambda = a$. For our choice of parameter values $v(a, \theta_0) \simeq 7.6$, which corresponds dimensionally to about $7.6\,\mathrm{cm\,s^{-1}}$. The average dimensional speed of the current across the width $-a < \lambda < a$ is about $4.4\,\mathrm{cm\,s^{-1}}$, which is qualitatively consistent with observations of, for example, the DWBC.

Figure 4 is a contour plot of the characteristics $\tau(\lambda, \theta)$ (or, equivalently, a contour plot of the stream lines $p(\lambda, \theta)$) in the (λ, θ)-plane for the τ-contours given by $\{-2 + n/2\}_{n=0}^{8}$. The up slope and down slope boundaries of the current are given by the $\tau = -2$ and 2 contours, respectively, and along these contours $h(\lambda, \theta) = 0$, i.e. they correspond to *groundings*. The current height is nonzero only in the gray-shaded region. The particle trajectories flow in the equatorward direction and and exhibit a slight westward tilt or shift as latitude decreases. Note that the streamlines corresponding to $\tau = -2$ and 2 (i.e. the up slope and down slope groundings) do not "tilt" westward and are therefore invariant with respect to latitude in accordance with (10b). The "crowding" of the interior stream lines near the up slope grounding is associated with an increase in the meridional speed of the current as it flows equatorward.

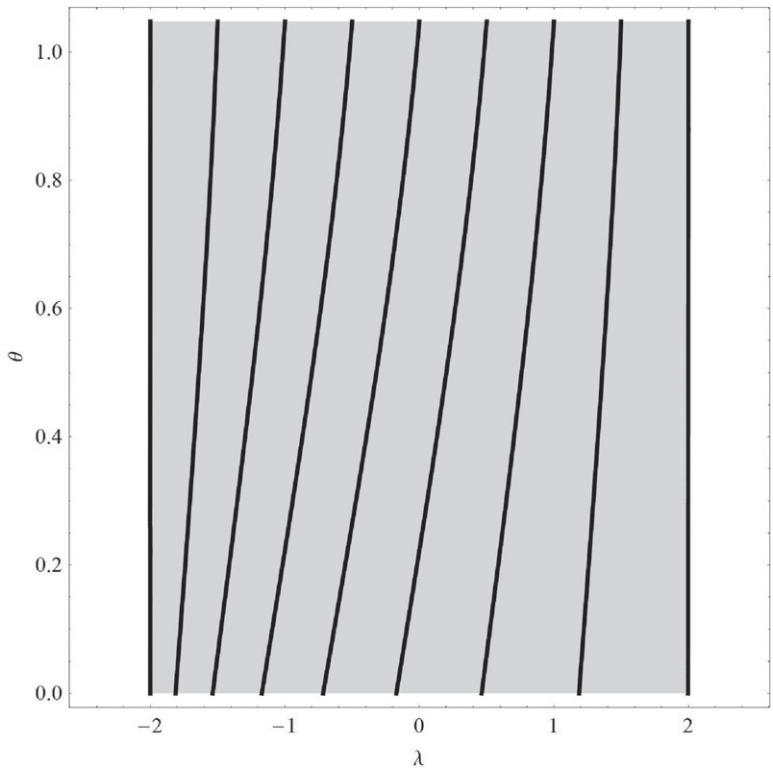

Figure 4. Contour plot of the characteristics/steam line $\tau\ (\lambda, \theta)$.

Figure 5(a) is a contour plot of $h(\lambda, \theta)$ in the (λ, θ)-plane. The h-contours are given by $\{n/5\}_{n=0}^{6}$ and a gray-scale shading is superimposed on the contour plot with *increasing* height associated with a *rdarkening* shade. The "outside" edge of the lightest gray-shaded region corresponds to where the abyssal height is grounded. While there is an approximately linear decrease in $h(\lambda, \theta)$ as the flow moves equatorward, this decrease is not uniform with respect to λ for a given θ. Physically, this is consequence of the slight westward or up slope component of the velocity throughout the solution, which leads to water gradually "piling" up along the up slope grounding as the flow proceeds equatorward.

The overall slightly super-linear decrease in $h(\lambda, \theta)$ as the flow moves equatorward can be seen in figure 5(b), which is graph of the zonally-averaged abyssal layer height, denoted by $\overline{h}(\theta)$, and given by

$$\overline{h}(\theta) \equiv \frac{1}{2a} \int_{-a}^{a} h(\lambda, \theta) \mathrm{d}\lambda, \tag{27}$$

for $0 \leq \theta \leq \theta_0$.

Figures 6(a) and (b) are contour plots of the meridional and zonal velocities $v(\lambda, \theta)$ and $u(\lambda, \theta)$, respectively, in the (λ, θ)-plane (θ is restricted to the region $0.15 \leq \theta \leq \theta_0$ to prevent contouring unbounded velocities). In figure 6(a) the v-contours are given by $\{-2n\}_{n=0}^{6}$ and in figure 6(b) the u-contours are given by $\{-2n\}_{n=0}^{4}$. In both figures 6(a)

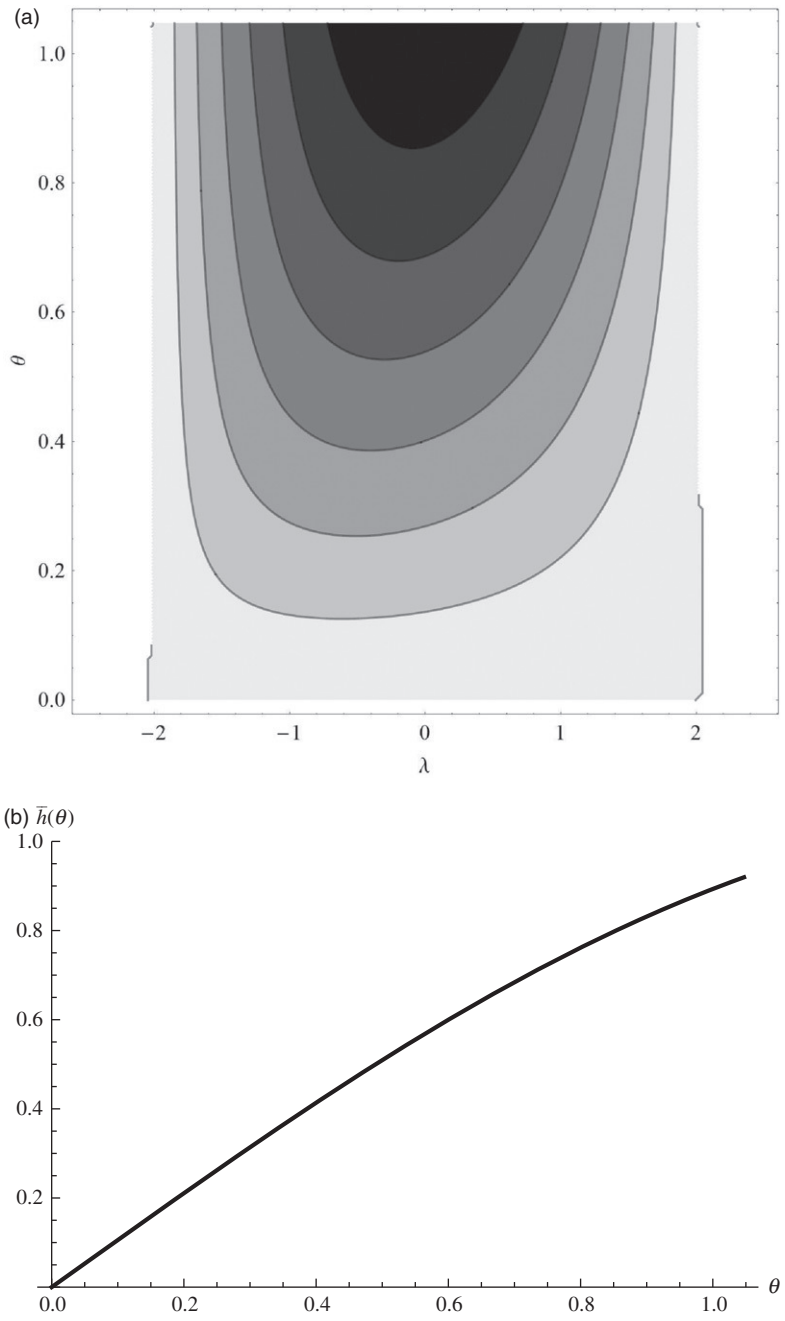

Figure 5. (a) Contour plot of the abyssal layer height $h(\lambda, \theta)$ in (λ, θ)-plane. (b) Graph of $\overline{h}(\theta)$ versus θ for $0 \leq \theta \leq \theta_0$.

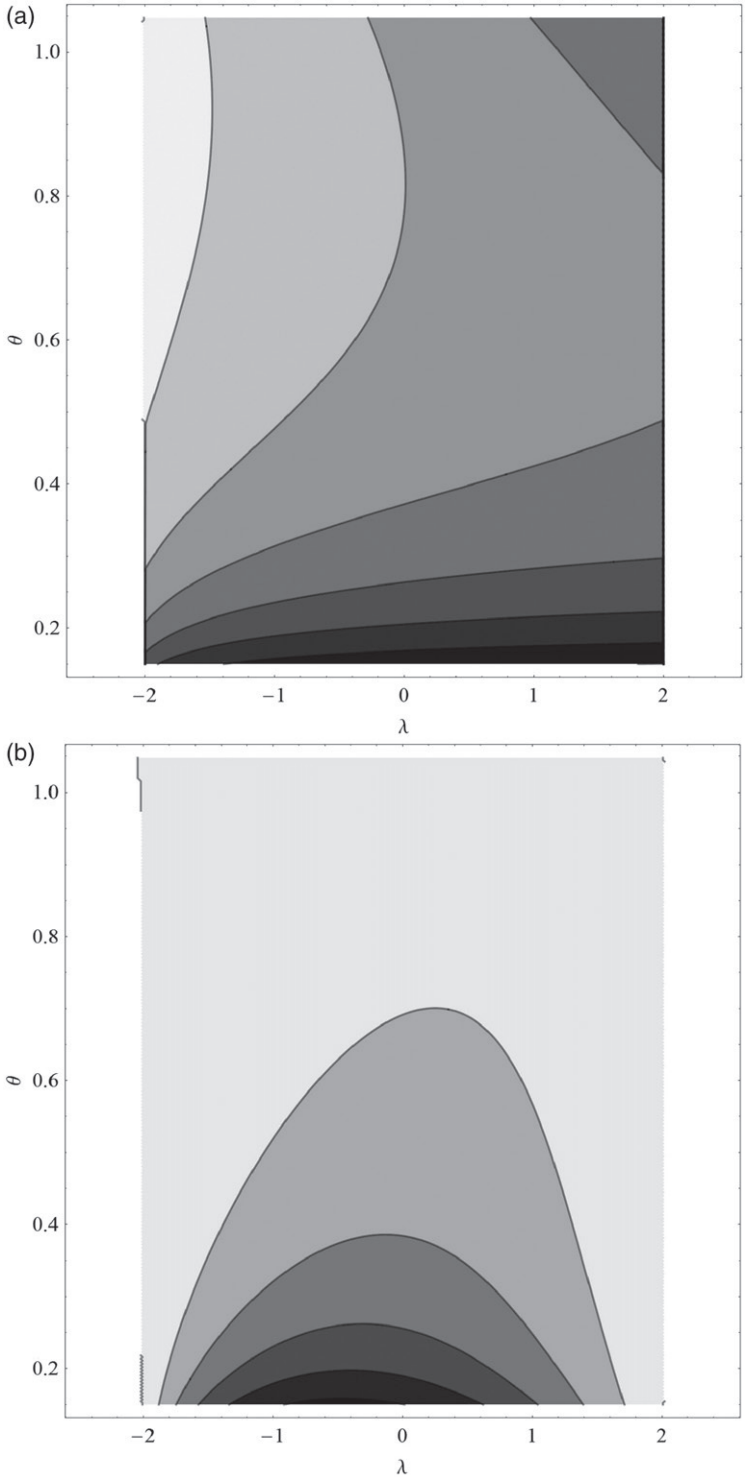

Figure 6. Contour plots of the velocities (a) $v(\lambda, \theta)$ and (b) $u(\lambda, \theta)$, respectively.

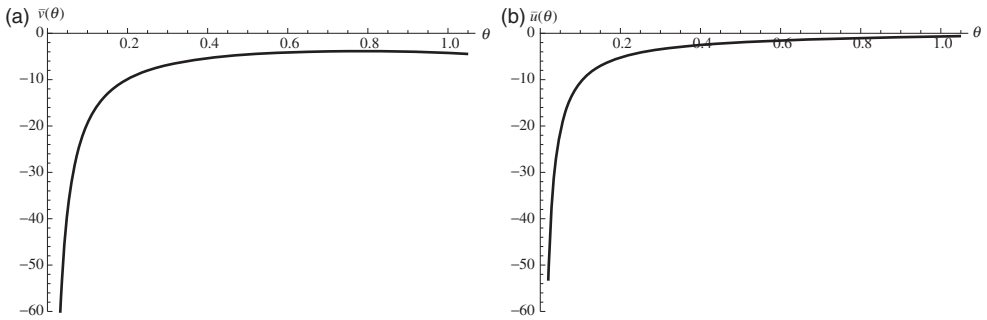

Figures 7. Graphs of the zonally-averaged velocities (a) $\overline{v}(\theta)$ and (b) $\overline{u}(\theta)$, respectively.

and (b) a gray-scale shading is superimposed on the contour plot, with *decreasing* velocity associated with a *darkening* shade. The velocities in both figures 6(a) and (b) are everywhere negative. The velocity $v(\lambda, \theta)$ along the "top" edge of figure 6a is exactly that shown in figure 3. From (2c,d), $v \simeq 1$ and $u \simeq 1$ corresponds, dimensionally, to about 1 and $0.02\,\mathrm{cm\,s^{-1}}$, respectively.

Figure 6(a) shows that meridional velocity is always equatorward and with the speed (averaged zonally over the current width) a few $\mathrm{cm\,s^{-1}}$ until about $\theta \simeq 0.2$ after which the velocity decreases rapidly as θ decreases toward the equator as a consequence of the $\sin\theta$ term in the denominator in (9b). Similarly, figure 6(b) shows that zonal velocity is always westward and with the speed (averaged zonally over the current width) of about $0.05\,\mathrm{cm\,s^{-1}}$ until towards about $\theta \simeq 0.2$ after which the velocity decreases rapidly as θ decreases the equator as a consequence of the $\sin\theta$ term in the denominator in (9a). Of course, the model looses any physical applicability in the limit $\theta \to 0$. The reason that velocities become, formally, unbounded as $\theta \to 0$ is the consequence of the fact that the planetary geostrophic model (4a–c) assumes the velocities are geostrophically given and the geostrophic approximation becomes singular at the equator. However, as we show below, since the steady-state version of (4c) is the statement that the horizontal divergence of the horizontal volume flux is zero, it will follow that the volume fluxes *uh* and *vh* are finite everywhere in the domain.

Figures 7(a) and (b) are graphs of the zonally-averaged meridional and zonal velocities $\overline{v}(\theta)$ and $\overline{u}(\theta)$, respectively, versus θ for $0.15 \le \theta \le \theta_0$, where

$$\overline{v}(\theta) \equiv \frac{1}{2a}\int_{-a}^{a} v(\lambda,\theta)\mathrm{d}\lambda, \quad \overline{u}(\theta) \equiv \frac{1}{2a}\int_{-a}^{a} u(\lambda,\theta)\mathrm{d}\lambda. \tag{28a,b}$$

We see in figures 7(a) and (b) the relatively slow variation of $\overline{v}(\theta)$ and $\overline{u}(\theta)$ as θ decreases until about $\theta \simeq 0.2$ after which the velocities decrease rapidly as θ decreases toward the equator (and the model loses applicability).

Figures 8(a) and (b) are contour plots of the meridional and zonal volume fluxes $v(\lambda,\theta)\,h\,(\lambda,\theta)$ and $u(\lambda,\theta)\,h\,(\lambda,\theta)$, respectively, in the (λ,θ)-plane over the entire $0 \le \theta \le \theta_0$ region. In figure 8(a) the *vh*-contours are given by $\{-n\}_{n=0}^{6}$ and in figure 8(b) the *uh*-contours are given by $\left\{-n/2\right\}_{n=0}^{5}$. In both figures 8(a) and (b) a gray-scale shading is superimposed on the contour plot, with *decreasing* volume flux associated with a *darkening* shade. The volume fluxes in both figures 8(a) and (b) are everywhere negative and finite. The volume fluxes do not become singular at the equator. The groundings

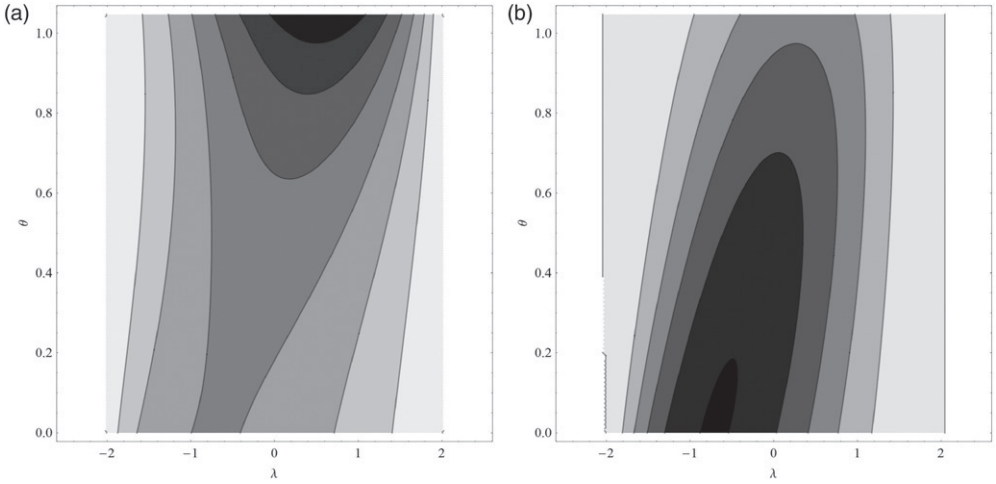

Figures 8. Contour plots of the fluxes (a) vh and (b) uh, respectively.

are located where the volume fluxes are zero. Dimensionally, $vh \simeq 1$ and $uh \simeq 1$ correspond to about 1.45 and $0.029\,\mathrm{m^2\,s^{-1}}$, respectively.

The (nondimensional) meridional volume transport associated with the abyssal flow as a function of latitude is obtained by integrating the meridional volume flux over the width of the current and is given by (11), i.e.

$$T_m(\theta) \equiv \int_{-a}^{a} h(\lambda,\theta)\, v(\lambda,\theta)\, \cos\theta\, \mathrm{d}\lambda = \frac{1}{\sin\theta_0} \int_{-a}^{a} h_0(\tau) h_B'(\tau) \mathrm{d}\tau,$$

which if (18a,b) is substituted in, yields,

$$T_m(\theta) = -\frac{-4\,H\,a\,s}{3\sin\theta_0} \simeq -8.18, \tag{29}$$

which is, of course, independent of θ. It follows from the scalings in (2a–f) that, dimensionally, $T_m \simeq 1$ corresponds to about $2\Omega V^2 L^2/g' \simeq 0.145\,\mathrm{Sv}$ ($1\,\mathrm{Sv} = 10^6\,\mathrm{m^3\,s^{-1}}$). Thus, for the model parameters chosen here, the abyssal current has associated with it an equatorward transport of about 1.2 Sv, which is consistent with observations of the ''deep'' transport associated with the ''overflow/lower deep water (LDW)'' near Cape Cod (see, e.g. figure 4 in Joyce *et al.* 2005). We hasten to add, however, that the equatorward transport for *entire lower* portion of the water column (including Labrador Sea Water (LSW)) as reported by Joyce *et al.* (2005), would put the transports an order of magnitude larger than the model estimate (29). However, Joyce *et al.*'s (2005) observations for DWBC near Cape Cod suggest that the dimensional thickness of the abyssal current should be several hundred metres and the width increased to about 300 km. Within the context of our simple idealized model, this would correspond to increasing H by a factor of about 5 and increasing a by about 1.5 and, based on (29), this will increase the computed volume transport to about 9 Sv, which is, again, consistent with Joyce *et al.'s* (2005) observations of the cumulative equatorward transport.

Although we are unaware of any direct observations of the zonal transport within these predominantly equatorward abyssal flows, the model predicts that the effects of planetary sphericity necessarily implies that a net nonzero zonal transport does occur even if, compared to the meridional transport, it is small. The net (nondimensional) zonal volume transport associated with the abyssal flow as a function of longitude, denoted here by $T_z(\lambda)$, is obtained by integrating the zonal volume flux over the latitudinal extent of the current, and is given by

$$\begin{aligned} T_z(\lambda) &\equiv \int_0^{\theta_0} h(\lambda,\theta)\, u(\lambda,\theta)\mathrm{d}\theta = -\int_0^{\theta_0} \frac{h\,(\lambda,\theta)\, p_\theta(\lambda,\theta)}{\sin\theta}\mathrm{d}\theta \\ &= -\frac{1}{\sin\theta_0}\int_0^{\theta_0} h_0(\tau)[h_0(\tau)+h_B(\tau)]_\tau \tau_\theta \,\mathrm{d}\theta \\ &= -\frac{1}{\sin\theta_0}\int_{\tau(\lambda,0)}^{\tau(\lambda,\theta_0)} h_{\,0}(\tau)\big[h_0'(\tau)+h_B'(\tau)\big]\mathrm{d}\tau \\ &= \frac{1}{\sin\theta_0}\left[\frac{h_0^2(\tau(\lambda,0))-h_0^2(\lambda)}{2} - \int_{\tau(\lambda,0)}^{\lambda} h_{\,0}(\tau)h_B'(\tau)\mathrm{d}\tau\right], \end{aligned} \tag{30}$$

where (6a,b) (noting that $\tau\,(\lambda,\theta_0)=\lambda$) and (8) has been used.

If (18a,b) is substituted into (30), we obtain

$$T_z = \frac{H}{\sin\theta_0}\left\{\frac{H}{a^2}\big[\lambda^2-\tau^2(\lambda,0)\big]\left[1-\frac{\lambda^2+\tau^2(\lambda,0)}{2a^2}\right]+s\left[\lambda-\tau(\lambda,0)+\frac{\tau^3(\lambda,0)-\lambda^3}{3a^2}\right]\right\}. \tag{31}$$

It follows from (31) that $T_z(\pm a)=0$ as it must, since the groundings, be located at $\lambda=\pm a$ are fixed and also streamlines and thus the normal velocity (given by u) and consequently the zonal transport T_z must be zero there. The zonal transport given by (31) is shown in figure 9, which is a graph of the net zonal volume transport $T_z(\lambda)$ for $-a\le\lambda\le a$. The zonal transport is everywhere negative indicating a westward,

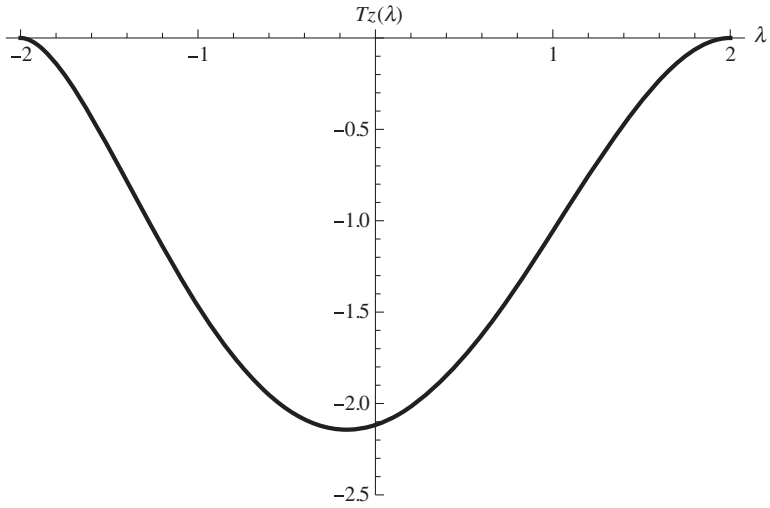

Figure 9. Graph of the net zonal volume transport $T_z(\lambda)$ for $-a\le\lambda\le a$.

or up slope, volume transport. It follows that, dimensionally, $T_z \simeq 1$ corresponds as well to about $2\Omega V^2 L^2/g' \simeq 0.145\,\mathrm{Sv}$. Thus, for the model parameters chosen here (representative of the deepest portion of the flow), the abyssal current has been associated with interior westward transports that range from 0 Sv along the groundings to about 0.29 Sv just slightly up slope from the line of longitude $\lambda = 0$. Even if a westward transport of 0.29 Sv seems appreciable, it is important to remember that: within the context of our model, this is occurring over a longitudinal arc of 60°, corresponding to a section that is about 6600 km long. The westward or up slope Eulerian velocities within the abyssal current are very small.

5. Summary

A report on a simple, but nevertheless illuminating, reduced-gravity shallow-water model for the meridional, or equatorward, flow of grounded abyssal currents on a longitudinally-sloping bottom on a rotating sphere has been given. For oceanographically relevant parameter values, it was shown that the abyssal layer height satisfies a quasi-linear hyperbolic equation with the velocities being geostrophically determined. The model corresponds to a planetary–geostrophic dynamical balance that permits the abyssal height field to intersect the bottom, i.e. a so-called grounding. Due to the fact that model is singular at the equator, it cannot be used to investigate cross-equatorial or inter-hemispheric flow. However, it was shown that the meridional and longitudinal volume fluxes are defined throughout the flow.

The steady-state limit of the equation governing the abyssal layer height could be solved exactly. For a physical configuration corresponding to flow in the northern hemisphere on topography associated with increasing ocean depth in the eastward direction, the abyssal current flows equatorward from the northeast to southwest direction. The characteristics associated with the quasi-linear hyperbolic model were shown to be co-parallel with the geostrophic streamlines. It was shown that the groundings could not vary with latitude and are therefore set by the northern boundary condition. The meridional volume transport was shown to be independent of latitude. Conditions for possible shock formation in the solution were established. Specially, it was shown that if the meridional velocity associated with the boundary condition on the abyssal layer height is everywhere equatorward (for a geometrical configuration corresponding to the flow of abyssal currents along the western edge of an ocean basin, e.g. the western north Atlantic), then no shock will form. If a shock does form, it is possible that this could lead to mixing on the up slope or western flank of these propagating abyssal water masses, which would be quite different than the instability and mixing associated with baroclinic destabilization. These and other issues require further study.

An example solution was described in which the abyssal layer height is parabolic in shape and possesses two groundings, one located on the up slope flank and one located on the down slope flank of the current. In this case, the characteristics, i.e. the streamlines were explicitly determined, and detailed descriptions of the along and cross-slope flow pathlines, the abyssal layer height as a function of longitude and latitude, the Eulerian velocity field within the abyssal, the meridional and zonal volume fluxes as well as the meridional and zonal volume transports were given.

Acknowledgements

Preparation of this paper was partially supported by the Natural Sciences and Engineering Research Council of Canada.

References

Anderson, D. and Killworth, P.D., Non-linear propagation of long Rossby waves. *Deep-Sea Res*. 1979, **26**, 1033–1050.

Charney, J.G. and Flierl, G.R., Oceanic analogues of large scale atmospheric motions. In *Evolution of Physical Oceanography - Scientific Surveys in Honor of Henry Stommel*, edited by B.A. Warren and C. Wunsch, pp. 504–548, 1981. (Massachusetts: MIT Press).

Choboter, P.F. and Swaters, G.E., Two layer models of abyssal equator crossing flow. *J. Phys. Oceanogr*. 2003, **33**, 1401–1415.

Choboter, P.F. and Swaters, G.E., Shallow water modeling of Antarctic Bottom Water crossing the equator. *J. Geophys. Res*. 2004, **109**, C03038.

Dewar, W.K., Planetary shock waves. *J. Phys. Oceanogr*. 1987, **17**, 470–482.

Edwards, C.A. and Pedlosky, J., Dynamics of nonlinear cross-equatorial flow. Part I: Potential vorticity transformation. *J. Phys. Oceanogr*. 1998a, **28**, 2382–2406.

Edwards, C.A. and Pedlosky, J., Dynamics of nonlinear cross-equatorial flow. Part II: The tropically enhanced instability of the western boundary current. *J. Phys. Oceanogr*. 1998b, **28**, 2407–2417.

Edwards, N.R., Willmott, A.J. and Killworth, P.D., On the role of topography and wind stress on the stability of the thermohaline circulation. *J. Phys. Oceanogr*. 1998, **28**, 756–778.

Joyce, T.M., Dunworth-Baker, J., Pickart, R.S. and Waterman, S., On the Deep Western Boundary Current south of Cape Cod. *Deep-Sea Res*. 2005, **52**, 615–625.

Nof, D., The translation of isolated cold eddies on a sloping bottom. *Deep-Sea Res*. 1983, **30**, 171–182.

Nof, D. and Borisov, S., Inter-hemispheric oceanic exchange. *Quart. J. Roy. Meteor. Soc*. 1998, **124**, 2829–2866.

Nof, D., Paldor, N. and van Gorder, S., The Reddy maker. *Deep-Sea Res*. 2002, **49**, 1531–1549.

Poulin, F.J. and Swaters, G.E., Sub-inertial dynamics of density-driven flows in a continuously stratified fluid on a sloping bottom. I. Model derivation and stability conditions. *Proc. Roy. Soc. Lond. A* 1999, **455**, 2281–2304.

Reszka, M.K., Swaters, G.E. and Sutherland, B.R., Instability of abyssal currents in a continuously stratified ocean with bottom topography. *J. Phys. Oceanogr*. 2002, **32**, 3528–3550.

Richardson, P.L., On the crossover between the Gulf Stream and the Western Boundary Undercurrent. *Deep-Sea Res*. 1977, **24**, 139–159.

Stommel, H. and Arons, A.B., On the abyssal circulation of the world ocean – I. Stationary flow patterns on a sphere. *Deep-Sea Res*. 1960, **6**, 140–154.

Swaters, G.E., On the baroclinic instability of cold-core coupled density fronts on sloping continental shelf. *J. Fluid Mech*. 1991, **224**, 361–382.

Swaters, G.E., Numerical simulations of the baroclinic dynamics of density-driven coupled fronts and eddies on a sloping bottom. *J. Geophys. Res*. 1998, **103**, 2945–2961.

Swaters, G.E., On the meridional flow of source-driven abyssal currents in a stratified basin with topography. Part I. Model development and dynamical characteristics. *J. Phys. Oceanogr*. 2006a, **36**, 335–355.

Swaters, G.E., On the meridional flow of source-driven abyssal currents in a stratified basin with topography. Part II. Numerical Simulation. *J. Phys. Oceanogr*. 2006b, **36**, 356–375.

Swaters, G.E., Mixed bottom-friction-Kelvin-Helmholtz destabilization of source-driven abyssal overflows in the ocean. *J. Fluid Mech*. 2009, **626**, 33–66.

Swaters, G.E. and Flierl, G.R., Dynamics of ventilated coherent cold eddies on a sloping bottom. *J. Fluid Mech*. 1991, **223**, 565–588.

Vallis, G.K., *Atmospheric and Oceanic Fluid Dynamics*, 2006. (New York: Cambridge University Press).

Wright, D.G. and Willmott, A.J., Buoyancy driven abyssal circulation in a circumpolar basin. *J. Phys. Oceanogr*. 1992, **22**, 139–154.

Appendix

The solution given by (6a,b) can be obtained as follows. The characteristic equations associated with (5a,b) may be written in the form

$$\frac{\mathrm{d}\theta}{\mathrm{d}\sigma} = \tan\theta \quad \text{subject to} \quad \theta|_{\sigma=0} = \theta_0, \tag{A.1a}$$

$$\frac{\mathrm{d}\lambda}{\mathrm{d}\sigma} = -\frac{h}{h_{B_\lambda}} \quad \text{subject to} \quad \lambda|_{\sigma=0} = \tau, \tag{A.1b}$$

$$\frac{\mathrm{d}h}{\mathrm{d}\sigma} = h \quad \text{subject to} \quad h|_{\sigma=0} = h_0(\tau), \tag{A.1c}$$

where (τ, σ) are the independent characteristic coordinates in which σ and τ are "along" and "across" the characteristics, respectively, in which τ is the parameter used in the parameterization of the boundary data/curve (5b), written in the form

$$h = h_0(\tau), \quad \lambda = \tau \quad \text{and} \quad \theta = \theta_0 \quad \text{along} \quad \sigma = 0. \tag{A.2}$$

The parameterization given by (A.2) may be considered as the "initial" condition associated with the characteristic equations (A.1a,c).

The solutions to the separable differential equations (A.1a,b) may be written in the form, respectively,

$$\frac{\sin\theta}{\sin\theta_0} = \mathrm{e}^{\sigma}, \quad h = h_0(\tau)\,\mathrm{e}^{\sigma}. \tag{A.3a,b}$$

Substituting (A.3b) into (A.1b) leads to

$$\frac{\mathrm{d}\lambda}{\mathrm{d}\sigma} = -\frac{h_0(\tau)\,\mathrm{e}^{\sigma}}{h_{B_\lambda}},$$

which can be integrated to yield

$$h_B(\lambda) - h_B(\tau) = h_0(\tau)(1 - \mathrm{e}^{\sigma}). \tag{A.4}$$

Finally, eliminating e^{σ} in (A.3b) and (A.4) using (A.3a) leads to

$$h = \frac{\sin\theta}{\sin\theta_0} h_0(\tau),$$

$$h_B(\lambda) = h_B(\tau) + \frac{\sin\theta_0 - \sin\theta}{\sin\theta_0} h_0(\tau),$$

which are (6a,b), respectively.